

1 **Harvesting of *Rhodotorula glutinis* via polyaluminium chloride or**
2 **cationic polyacrylamide using the extended DLVO theory**

3 Peng Yin¹, Tong Yu², Hujun Liu¹, Xu Zhang^{*2}, Tianwei Tan²

4 1 Academy of National Food and Strategic Reserves Administration, No.11 Bai wan
5 zhuang street, Xicheng District, Beijing, 100037, PR China.

6 2 Beijing Key Lab of Bioprocess, National Energy R&D Center for Biorefinery,
7 College of Life Science and Technology, Beijing University of Chemical Technology,
8 Beijing 100029, PR China.

9 Email: 17801197735@163.com;

10 **Abstract:** Polyaluminium chloride (PAC) and cationic polyacrylamide (CPAM)
11 play a crucial role for separating microorganisms from bulk media. However, the
12 mechanism of adsorption between cells and flocculants remain to be further defined to
13 improve the flocculation efficiency (FE) in extreme conditions. This study conducted
14 the flocculation process of *Rhodotorula glutinis* induced by PAC and CPAM, firstly.
15 The result demonstrated that CPAM possessed more efficient harvesting ability for *R.*
16 *glutinis* compared to PAC. The difference of flocculation capacity was then
17 thermodynamically explained by the extended DLVO (eDLVO) theory, it turned out
18 that the poor harvesting efficiency of PAC was attributed to lacking of binding sites as
19 well as low adsorption force within particles. Based on this, the FE of PAC to *R.*
20 *glutinis* was mechanically enhanced to 99.84% from 32.89% with 0.2 g/L CPAM

21 modification at an optimum pH of 9.

22 **Keywords:** Flocculation; *Rhodotorula glutinis*; The extended DLVO theory;
23 Polyaluminium chloride; Cationic polyacrylamide

24 * Corresponding author. E-mail: zhangxu@mail.buct.edu.cn

25 1. Introduction

26 Biofuels and Biodiesel, as one type of renewable and sustainable resources, were
27 proposed to alleviate the global energy crisis sharpened due to resource starvation as
28 well as the aggravation of environmental pollution. Oleaginous microorganisms,
29 generally represented by algae and some of yeasts, such as *Chlorella vulgaris*, and
30 *Rhodotorula glutinis*, were regarded as one of the most promising feedstocks to
31 produce biofuels since the properties of low costs, high productivity and accessible
32 culture conditions (Zhao et al. 2008; Dong et al. 2013; Razack et al. 2016). In the
33 wholesale biofuels production from microbes, biomass harvesting is one critical part
34 when taking the cost proportion into consideration. Horiuchi et al. (2003) concluded
35 that the cost of harvesting process could account for up to 30% of the whole
36 production resulting from the small cell size and the stable surface charge (Horiuchi et
37 al. 2003; Powell et al. 2013). Thus, an efficient approach for harvesting oleaginous
38 microbes is urgent to promote efficient biomass harvesting.

39 Flocculation, broadly regarded as the most promising pretreatment approach, has
40 promptly developed as the optimum candidate of separation techniques (Vandamme et
41 al. 2013), while other traditional techniques, such as centrifugation, gravity
42 sedimentation, flotation, and membrane filtration, was turned out to be time and

43 energy consuming (Milledge et al. 2013). Therefore, various chemical flocculants
44 have been synthesized and improved to meet the demand of economic concepts and
45 safety standard (Gerde et al. 2014; Gupta et al. 2014). Besides, the cost effective
46 inorganic and organic flocculants, represented by PAC and CPAM, still attracted
47 much attention and was widely utilized in the large-scale biomass harvesting when the
48 problem of secondary contaminant could be ignored (Wang et al. 2015; Zhao et al.
49 2015). In general, the pleased flocculation efficiency mainly attributes to repeating
50 optimization of conditions or even the surface modification of particles. Therefore, the
51 understanding of flocculation mechanism was essential to improve the flocculation
52 efficiency purposefully.

53 The interactions, involved in the flocculation process, were generally considered as
54 the combination of electrostatic adsorption, bridging, and netting (Li et al. 2018).
55 Several attempts have been made for explaining the flocculation process. Lartiges et
56 al. (1997) proposed the flocculation process was firstly triggered by the surface
57 anchoring, then stabilized to form pellets by the interactions aforementioned (Lartiges
58 et al. 1997). Bhattacharya et al. developed a mathematical model to describe the algal
59 harvesting process (Bhattacharya et al. 2017). The extended Derjaguin-Landau-
60 Verwey-Overbeek (eDLVO) theory, composed of Lifshitz-van der Waals interaction,
61 electrostatic interactions and Lewis acid-base interaction, was applied to
62 quantitatively determine the adsorption potentials within two particles (Van Oss.
63 2006). The eDLVO theory have been successfully utilized to explain the interaction
64 energy and attachment of microbial cells and solid substrate, such as the adsorption
65 between extracellular polymeric substance fractions and microbes (Xu et al. 2016),
66 interaction between microalgae and microfiltration membrane (Ahmad et al. 2013),

67 and adhesion of cells to particles (Agbakpe et al. 2014).

68 In this study, the soluble flocculants CPAM and PAC were utilized to flocculate *R.*
69 *glutinis*. The specific objectives are (1) to conduct the flocculation process and
70 compare the FE, (2) to thermodynamically explain the difference of FE via the
71 eDLVO, (3) to enhance the unsatisfied FE of PAC for *R. glutinis* based on the
72 analyses.

73 **2. Materials and Methods**

74 **2.1. Oleaginous strains and culture conditions**

75 The yeast of *R. glutinis* (CGMCC No. 2258), used to produce flocculation process,
76 was provided by the China National Research Institute of Food and Fermentation
77 Industries and stored in the Beijing University of Chemical Technology. The
78 cultivation medium (Xue et al. 2008) was made by dissolving 40 g glucose, 1.5 g
79 yeast extract powder, 7 g KH_2PO_4 , 2 g $(\text{NH}_4)_2\text{SO}_4$, 2 g MgSO_4 , 2 g Na_2SO_4 in 1 L
80 deionized water, autoclaved at 116°C for 25 min, and cultivated in 500 mL
81 Erlenmeyer flasks with 100 mL medium at 30°C, 180 r/min. The microorganisms
82 were harvested after 96 h cultivation with the final concentration being 16.92 g dry
83 weight/L.

84 **2.2. Flocculation experiment**

85 **2.2.1. Concentration effect of PAC and CPAM on FE**

86 PAC and CPAM, provided by a vendor (Lablead Corp, China), were utilized as the
87 flocculants. The flocculation processes were conducted in 50 mL centrifuge tubes

88 with 20 mL medium volume. The cell suspension mixed with the flocculants was
89 thoroughly stirred by the magnetic stirrer at the speed of 900 r/min for 90 s and
90 lowered to 200 r/min for 30 s and then left standing for 10 min. OD₆₀₀ for the
91 suspension obtained from 80% height of the mixture were determined.

92 2.2.2. pH induced flocculation

93 The pH of the cell culture solution was adjusted with 1 mol/L H₂SO₄ and NaOH.
94 Then the desired flocculants were added into the cell suspension and the flocculation
95 processes were performed under conditions as described in 2.2.1.

96 2.2.3. CPAM modified flocculation

97 The CPAM solution was made by dissolving 0.1 g CPAM in 100 mL DI water. The
98 CPAM solution was added to cell suspension to obtain the CPAM modified *R. glutinis*
99 cells. Then PAC was added in the mixture and the flocculation experiment was
100 conducted under conditions as described in 2.2.1.

101 2.3. Characterization

102 The size distributions of *R. glutinis* were determined by the Dynamic Light
103 Scattering (DLS) technique (Brookhaven Instrument Corp, USA). In this study, the
104 adsorption between cells and the flocculants was assumed as the interaction between
105 cells and the cells coated with flocculants. Thus, the diameters of the soluble
106 flocculants were equal with the average diameter of *R. glutinis*.

107 The zeta potentials of *R. glutinis* suspension were directly measured by a zeta
108 potential analyzer (Brookhaven Instrument Corp, USA). The zeta potentials of

109 flocculants were calculated using standard curve that described the relationship
110 between zeta potentials and the dosage.

111 The contact angles of particles and water, ethylene glycol and α -bromonaphthalene
112 were determined by DSA 100 system (Powereach Inc., China).

113 2.4. Harvesting efficiency evaluation

114 The flocculation efficiency (FE) and harvesting efficiency (HE) were used to
115 evaluate the flocculation performance and calculated according to Eq. (1) (Hu et al.
116 2013) and Eq. (2):

$$117 \quad FE(\%) = \left[1 - \frac{OD_n}{OD_0} \right] \times 100\% \quad (1)$$

$$118 \quad HE(\%) = \frac{V_n}{V_0} \times 100\% \quad (2)$$

119 where OD_0 and OD_n mean OD values measured before and after flocculation process
120 at the optical density of 600 nm; V_n was the volume of aggregated microbes, and V_0
121 was the initate volume of cell culture.

122 3. Results and Discussion

123 3.1. Comparison of CPAM and PAC for harvesting *R. glutinis*

124 The concentration influences of PAC and CPAM on flocculating results of *R.*
125 *glutinis* were conducted and the result was shown in **Fig. 1**. As shown in **Fig. 1a**, with
126 CPAM dosage range of 0.1-0.3 g/L, the flocculation efficiency of *R. glutinis* increased
127 while the increment speed decreased. Besides, the maximum FE (99.75%) was

obtained with the concentration of CPAM being 0.3 g/L . Subsequently, FE showed a downward trend with the increment of CPAM. The above relationship between FE and the flocculant dosage was explained by the adsorption process within cells and flocculants. Firstly, the number of cells adsorbed is increasing with the concentration of flocculant increment, so the FE showed an upward trend. However, the flocculant would be added to stabilize the flocculation system again when the dosage of flocculant and the number of cells reached the state of saturated adsorption, and the further addition of the flocculants contributed to the reducing FE. Besides, HE also showed a certain variation with the increment of flocculants. Within the range of 0.1-0.3 g/L, HE increased as the amount of cells adsorbed by the flocculant increased with the flocculation efficiency increased. And the maximum HE (18.67%) was obtained when the dosage of CPAM being 0.3 g/L. Therefore, 0.3 g/L was considered as the optimal concentration of CPAM when flocculating *R. glutinis*.

The effect of PAC concentration on the FE and HE of *R. glutinis* was presented in **Fig. 1b**. The FE showed a steady upward trend at a flocculant dosage scope of 0.4-1.6 g/L, and the maximum FE (32.89%) was obtained when the flocculant dosage being 1.6 g/L. Further addition of PAC did not significantly increase FE compared with 1.6 g/L addition. In addition, HE increased with the addition of PAC, and it reached up to 63.64% when PAC addition being 2.0 g/L. This suggested that additional dosage of PAC, more than 1.6 g/L, contributed little increasement to the FE but resulted in a sharp increment of HE. Thus, the PAC dosage of 1.6 g/L was chosen throughout the whole flocculation experiment of *R. glutinis*.

It was derived that CPAM induced flocculation was more efficient to *R. glutinis* than PAC. The eDLVO theory, utilized to analyze the interaction energies involved in the flocculation process, was applied to explore the difference of the flocculation results mentioned above.

3.2. Explanation of flocculation differences with the eDLVO theory

Table 1 listed the contact angles of the flocculants and cells with water, ethylene glycol and α -bromonaphehalene (surface energy components given in **Table 2**) (Good and Oss 1992). The surface energy components (γ_s^{LW} , γ_s^{+dd} and γ_s^{-dd}) of particles (shown in **Table 3**) were calculated according to Eq. (3) (Dann 1970).

The amount of flocculant addition was proportional to the surface area of the cell, and the zeta potential was proportional to the charge of the cell surface. Thus, there existed a linear relationship between the zeta potential and flocculant concentration (shown in **Fig. 2**) and written as :

$$y = 0.00176 + 0.01167 x \quad (3)$$

$$y = -0.0424 + 0.2279 x \quad (4)$$

where unit of x was mg in Eq.(3), while μg in Eq.(4). The calculated zeta potentials were calculated using optimum concentration based on the abovementioned assumption and the results were summarized in **Table 1**.

In the follow model the cells were assumed as spheres (Zhang, X. et al. 2019) and the flocculants completely covered the surface of the yeast. Therefore, the interactions

between the cells and the flocculants were modeled as particle-particle geometry.

The Lifshitz-van der Waals interaction and Lewis acid-base interaction of cells and the flocculants were derived from Eq.(6) and (7).

$$(1+\cos\theta)\gamma_l=2\gamma_{lv} \quad (5)$$

$$\Delta G_{mws}^{LW}=-2\left(\sqrt{\gamma_{mv}^{LW}}-\sqrt{\gamma_{lv}^{LW}}\right)\left(\sqrt{\gamma_{sv}^{LW}}-\sqrt{\gamma_{lv}^{LW}}\right) \quad (6)$$

$$\Delta G_{mws}^{AB}=2\gamma_{mv}^+ \gamma_{lv}^- - 2\gamma_{sv}^+ \gamma_{lv}^- \quad (7)$$

In view of their spherical shapes, the Lifshitz-van der Waals interaction and Lewis acid-base interaction separated by distance d can be written as:

$$\Delta G^{LW}(d)=\frac{-Ar}{12d} \quad (8)$$

$$A=-12\pi d_0^2 \Delta G_{mws}^{LW} \quad (9)$$

$$\Delta G^{AB}(d)=\pi r \lambda \Delta G_{mws}^{AB} \exp\left[\left(d_0-d\right)/\lambda\right] \quad (10)$$

where A was the Hamaker constant; λ was the correlation length and d_0 was the closest distance between two particles. The values of λ and d_0 were given being 0.6 nm and 0.157 nm, respectively (Van Oss 2006).

Formula 11 expresses the electrostatic interaction energy separated by distanced (Van Oss et al. 1986):

$$\Delta G^{EL}(d)=\frac{\pi\epsilon r\left(\zeta_1^2+\zeta_2^2\right)}{2}\left[\frac{2\zeta_1\zeta_2}{\zeta_1^2+\zeta_2^2}\ln\frac{1+\exp(-\kappa d)}{1-\exp(-\kappa d)}+\ln\left(1-\exp(-2\kappa d)\right)\right] \quad (11)$$

where ζ and ϵ were the zeta potential and permittivity of the medium, respectively; κ^{-1} was the double-layer thickness and can be found out as:

$$\kappa^{-1} = \sqrt{\frac{\epsilon k T}{e^2 \sum v_i^2 n_i}} \quad (12)$$

where k was Boltzmann's constant and being 1.38×10^{-23} J/K; e was charge of an electron and being 1.60×10^{-19} C; T was absolute temperature and being 298.15 K; n_i was the number density of different ions in the bulk liquid; v_i was the corresponding valency. In this study, κ^{-1} of *R. glutinis* cultural was calculated to be 1.1862 nm.

The eDLVO theory (Van Oss 2006) proposed that the total Gibbs free energy (

ΔG_{TOT}) was consisted of ΔG^{LW} , ΔG^{AB} and ΔG^{EL} . The variation of ΔG_{TOT} , ΔG^{LW} ,

ΔG^{AB} and ΔG^{EL} versus the separation distance d between cells and ISMM were

plotted in **Fig. 3**.

It was demonstrated that ΔG_{TOT} between *R. glutinis* and the flocculants showed a primary minimum and totally attractive force due to the negative ΔG^{LW} , ΔG^{AB} and

ΔG^{EL} . However, *R. glutinis* showed a preference to CPAM than PAC as ΔG_{TOT}

between CPAM and cells was stronger than PAC. As for CPAM, ΔG_{TOT} was negative

and presented attract interaction, which was in accordance with the satisfied

flocculation results shown in **Fig. 1a**. The negative interaction between PAC and *R.*

glutinis indicated that PAC was potential to attractive the yeast, which was

inconsistent with the poor flocculation efficiency (shown in **Fig. 1b**). The conflict

may attribute to the insufficient binding sites between PAC and cells, thus the

flocculation process was not completely triggered. Besides, the lower zeta potential between cells and PAC contributed to the weaker electrostatic interaction.

3.3. Enhancement of PAC for harvesting *R. glutinis*

The pH induced flocculation of *R. glutinis* cells with PAC was performed because the surface charge of the yeast could be changed in different pH conditions. As apparent in **Fig.4**, PAC showed poor flocculation efficiency of *R. glutinis* (the flocculation efficiencies were 44.52%, 45.2% and 45.86% at pH 3, 5 and 7, respectively) when the pH value was in the range of 3-7. The HE decreased from 61.22% to 51.15%. When the pH was 9, the FE increased to 57.24%, and the corresponding HE was 52.27%. The FE was enhanced with the pH value further increasing, and HE reduced slightly. It was derived that the optimum pH value for PAC flocculating *R. glutinis* was 9, and the FE and HE were 57.24% and 52.27%, respectively.

Based on the results above, the FE could be improved further by enhancing the surface complexing interaction between *R. glutinis* cells and PAC. CPAM was chosen to modify *R. glutinis* cells as it not only adsorbed to cells but also increased the amount of -OH of cells after adsorption. The harvesting results were sharply improved and when flocculated *R. glutinis* modified with different amounts of CPAM via PAC (shown in **Table 4**). The FE was as high as 99.84% when the concentration of CPAM and PAC being 0.2 g/L and 0.4 g/L, respectively. And the HE was only 19.34% in this condition. While the optimal FE (32.89%) was obtained when conducting PAC induced flocculation, and the corresponding HE reached up to

229 63.64%. Thus, it can be concluded that the modification with CPAM can significantly
230 reduce the amount of flocculants and improve the flocculation results.

231 **4. Conclusions**

232 CPAM showed satisfied harvesting efficiency to *R. glutinis* and the optimal FE and
233 HE were 99.75% and 18.67%, respectively. However, PAC was inefficient when
234 utilized to harvest *R. glutinis*, and the optimal FE was 32.89% with the dosage scope
235 being 0.4-2.0 g/L. The eDLVO theory was used to explain the difference between
236 CPAM and PAC, it was concluded that the poor flocculation ability of PAC to *R.*
237 *glutinis* was attributed to the lacking of binding sites and weak electrostatic
238 interaction. The FE was improved to 57.24% when pH value being 9.0, and the
239 corresponding HE being 52.27%. The flocculation efficiency was further enhanced by
240 CPAM modification, the FE and HE were 99.84 and 19.34% with the dosage of
241 CPAM and PAC being 0.2 g/L and 0.4 g/L, respectively.

242 **Acknowledgments**

243 The authors wish to express their thanks for the supports from the National Key
244 Research and Development Program of China (2017YFB0306800) and the 111
245 project (B13005).

246 **References**

247 Zhao, X., Kong, X., Hua, Y., Feng, B., & Zhao, Z. (2008). Medium optimization for
248 lipid production through co-fermentation of glucose and xylose by the
249 oleaginous yeast *Lipomyces starkeyi*. *European Journal of Lipid Science and*

250 Technology, 110(5), 405-412.

251 Dong, T., Wang, J., Miao, C., Zheng, Y., & Chen, S. (2013). Two-step in situ
252 biodiesel production from microalgae with high free fatty acid content.
253 Bioresource Technology, 136, 8-15.

254 Razack, S. A., Duraiarasan, S., & Mani, V. (2016). Biosynthesis of silver
255 nanoparticle and its application in cell wall disruption to release carbohydrate
256 and lipid from *C. vulgaris* for biofuel production. Biotechnology Reports, 11, 70-
257 76.

258 Horiuchi, J. I., Ohba, I., Tada, K., Kobayashi, M., Kanno, T., & Kishimoto, M.
259 (2003). Effective cell harvesting of the halotolerant microalga *Dunaliella*
260 *tertiolecta* with pH control. Journal of bioscience and bioengineering, 95(4), 412-
261 415.

262 Powell, R. J., & Hill, R. T. (2013). Rapid aggregation of biofuel-producing algae by
263 the bacterium *Bacillus* sp. strain RP1137. Appl. Environ. Microbiol., 79(19),
264 6093-6101.

265 Vandamme, D., Foubert, I., & Muylaert, K. (2013). Flocculation as a low-cost
266 method for harvesting microalgae for bulk biomass production. Trends in
267 biotechnology, 31(4), 233-239.

268 Milledge, J. J., & Heaven, S. (2013). A review of the harvesting of micro-algae for
269 biofuel production. Reviews in Environmental Science and Bio/Technology,
270 12(2), 165-178.

271 Gerde, J. A., Yao, L., Lio, J., Wen, Z., & Wang, T. (2014). Microalgae flocculation:

272 impact of flocculant type, algae species and cell concentration. *Algal research*, 3,
273 30-35.

274 Gupta, S. K., Kumar, M., Guldhe, A., Ansari, F. A., Rawat, I., Kanney, K., & Bux,
275 F. (2014). Design and development of polyamine polymer for harvesting
276 microalgae for biofuels production. *Energy conversion and management*, 85,
277 537-544.

278 Wang, C., Alpatova, A., McPhedran, K. N., & El-Din, M. G. (2015).
279 Coagulation/flocculation process with polyaluminum chloride for the
280 remediation of oil sands process-affected water: performance and mechanism
281 study. *Journal of environmental management*, 160, 254-262.

282 Zhao, Y., Liang, W., Liu, L., Li, F., Fan, Q., & Sun, X. (2015). Harvesting *Chlorella*
283 *vulgaris* by magnetic flocculation using Fe₃O₄ coating with polyaluminium
284 chloride and polyacrylamide. *Bioresource technology*, 198, 789-796.

285 Li, Y., Xu, Y., Zheng, T., & Wang, H. (2018). Amino acids in cell wall of Gram-
286 positive bacterium *Micrococcus* sp. hsn08 with flocculation activity on *Chlorella*
287 *vulgaris* biomass. *Bioresource technology*, 249, 417-424.

288 Lartiges, B. S., Bottero, J. Y., Derrendinger, L. S., Humbert, B., Tekely, P., & Suty,
289 H. (1997). Flocculation of colloidal silica with hydrolyzed aluminum: an ²⁷Al
290 solid state NMR investigation. *Langmuir*, 13(2), 147-152.

291 Bhattacharya, A., Malik, A., & Malik, H. K. (2017). A mathematical model to
292 describe the fungal assisted algal flocculation process. *Bioresource technology*,
293 244, 975-981.

294 Van Oss, C. J. (2006). Interfacial forces in aqueous media. CRC press.

295 Xu, J., Yu, H. Q., & Li, X. Y. (2016). Probing the contribution of extracellular
 296 polymeric substance fractions to activated-sludge bioflocculation using particle
 297 image velocimetry in combination with extended DLVO analysis. Chemical
 298 Engineering Journal, 303, 627-635.

299 Ahmad, A. L., Yasin, N. M., Derek, C. J. C., & Lim, J. K. (2013). Harvesting of
 300 microalgal biomass using MF membrane: kinetic model, CDE model and
 301 extended DLVO theory. Journal of membrane science, 446, 341-349.

302 Agbakpe, M., Ge, S., Zhang, W., Zhang, X., & Kobylarz, P. (2014). Algae
 303 harvesting for biofuel production: influences of UV irradiation and
 304 polyethylenimine (PEI) coating on bacterial biocoagulation. Bioresource
 305 technology, 166, 266-272.

306 Xue, F., Miao, J., Zhang, X., Luo, H., & Tan, T. (2008). Studies on lipid production
 307 by *Rhodotorula glutinis* fermentation using monosodium glutamate wastewater
 308 as culture medium. Bioresource technology, 99(13), 5923-5927.

309 Hu, Y. R., Wang, F., Wang, S. K., Liu, C. Z., & Guo, C. (2013). Efficient harvesting
 310 of marine microalgae *Nannochloropsis maritima* using magnetic nanoparticles.
 311 Bioresource technology, 138, 387-390.

312 Good, R. J., & van Oss, C. J. (1992). The modern theory of contact angles and the
 313 hydrogen bond components of surface energies. In Modern approaches to
 314 wettability (pp. 1-27). Springer, Boston, MA.

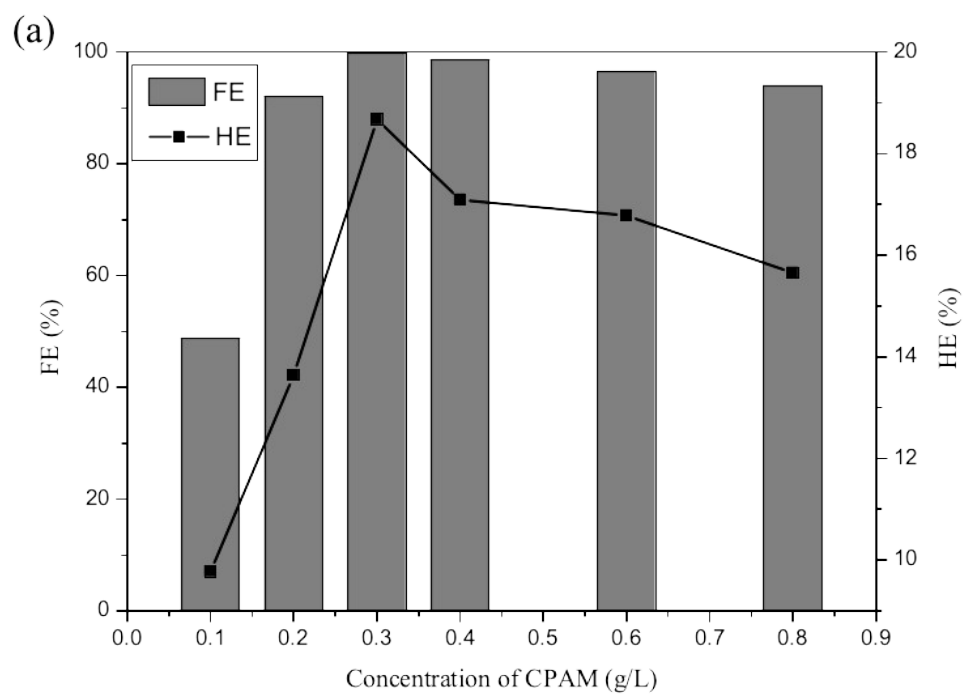
315 Dann, J. R. (1970). Forces involved in the adhesive process: I. Critical surface

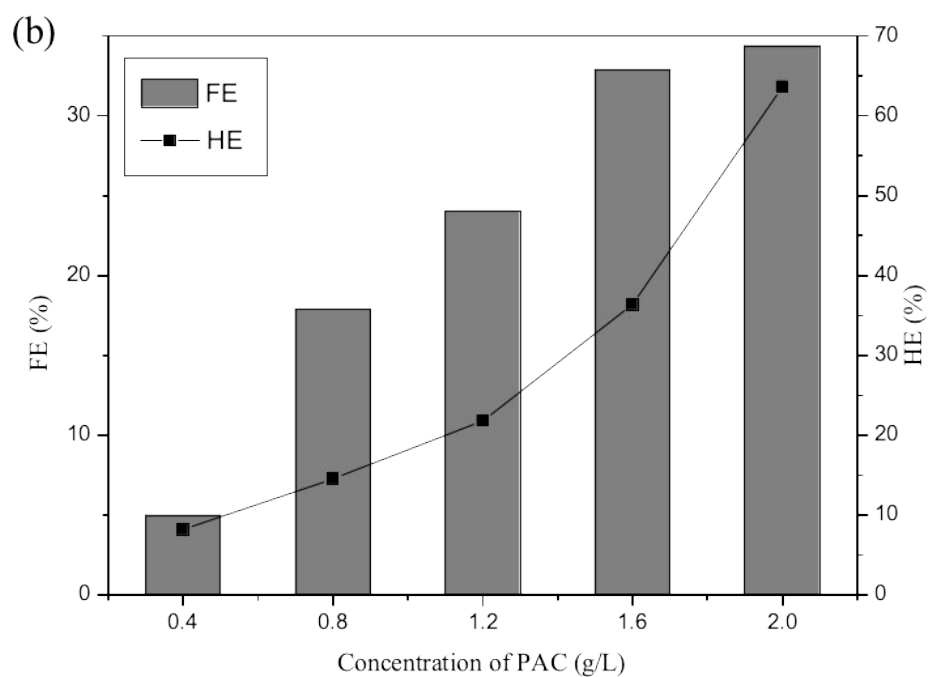
tensions of polymeric solids as determined with polar liquids. Journal of Colloid
and Interface Science, 32(2), 302-320.

Zhang, X., Zhou, X., Xi, H., Sun, J., Liang, X., Wei, J., ... & Chen, Y. (2019).
Interpretation of adhesion behaviors between bacteria and modified basalt fiber
by surface thermodynamics and extended DLVO theory. Colloids and Surfaces
B: Biointerfaces, 177, 454-461.

Van Oss, C. J., Good, R. J., & Chaudhury, M. K. (1986). The role of van der Waals
forces and hydrogen bonds in “hydrophobic interactions” between biopolymers
and low energy surfaces. Journal of colloid and Interface Science, 111(2), 378-
390.

List of figures

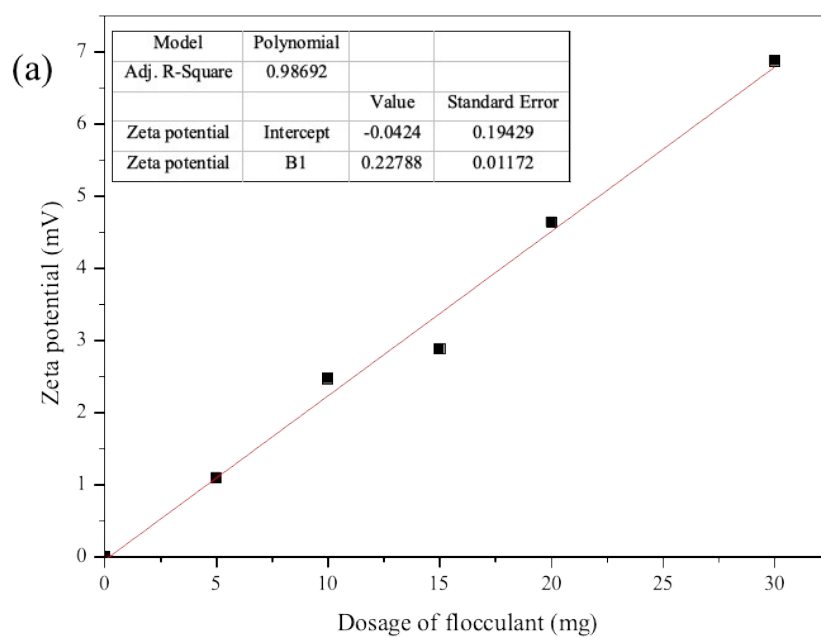




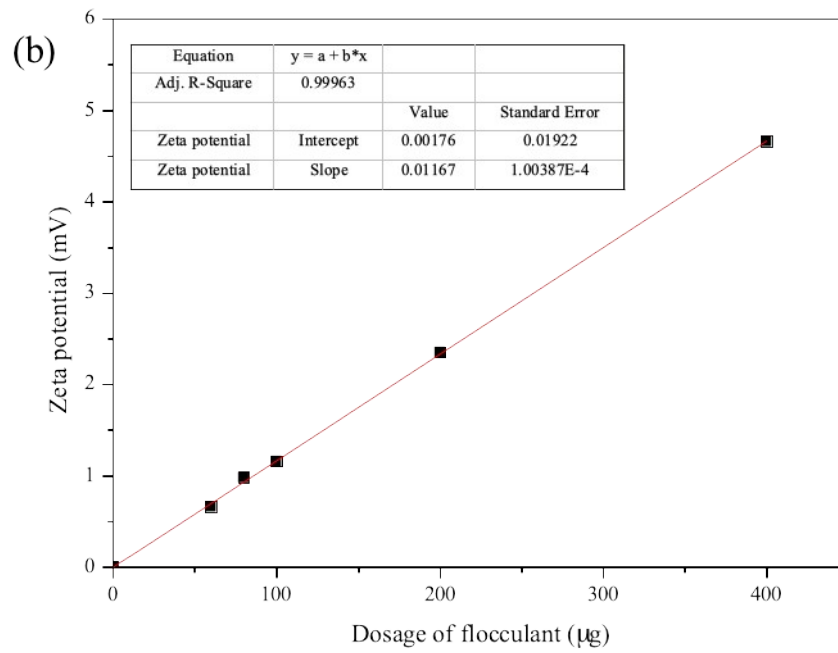
336

337 **Fig. 1.** Influence of flocculants concentration on FE and HE (a: CPAM and *R. glutinis*; b:

338 PAC coated *R. glutinis*)



339

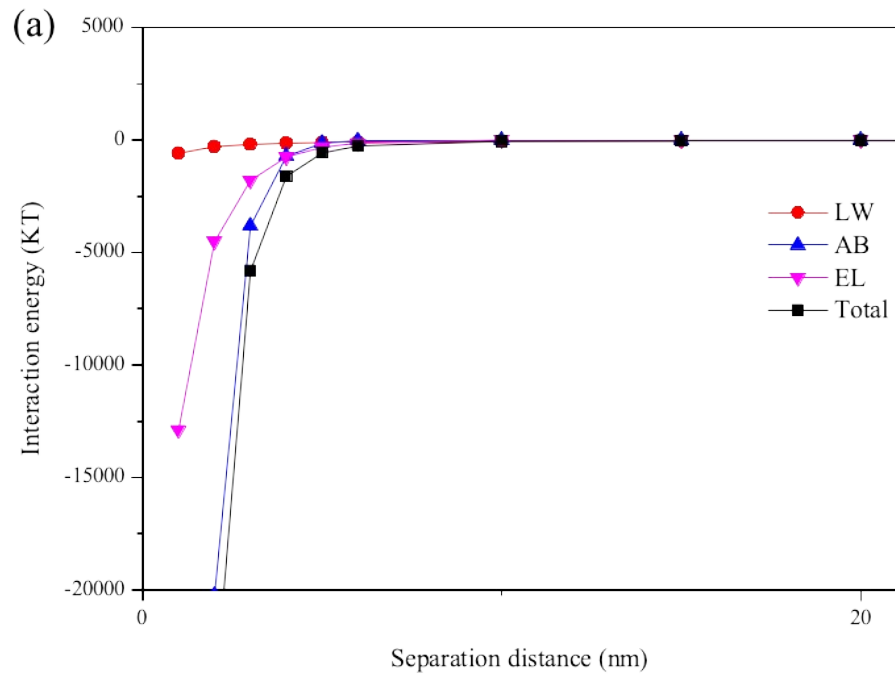


340

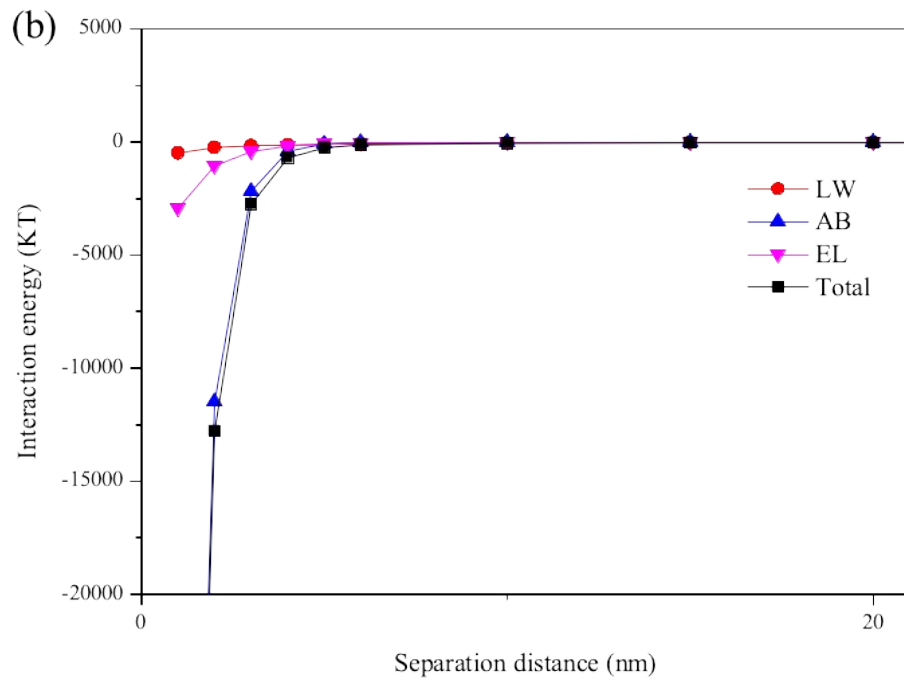
Fi

341 **g. 2.** Influence of concentration on zeta potential of PAC and CPAM in different culture (a: PAC
 342 coated *R. glutinis*; b: CPAM coated *R. glutinis*)

343



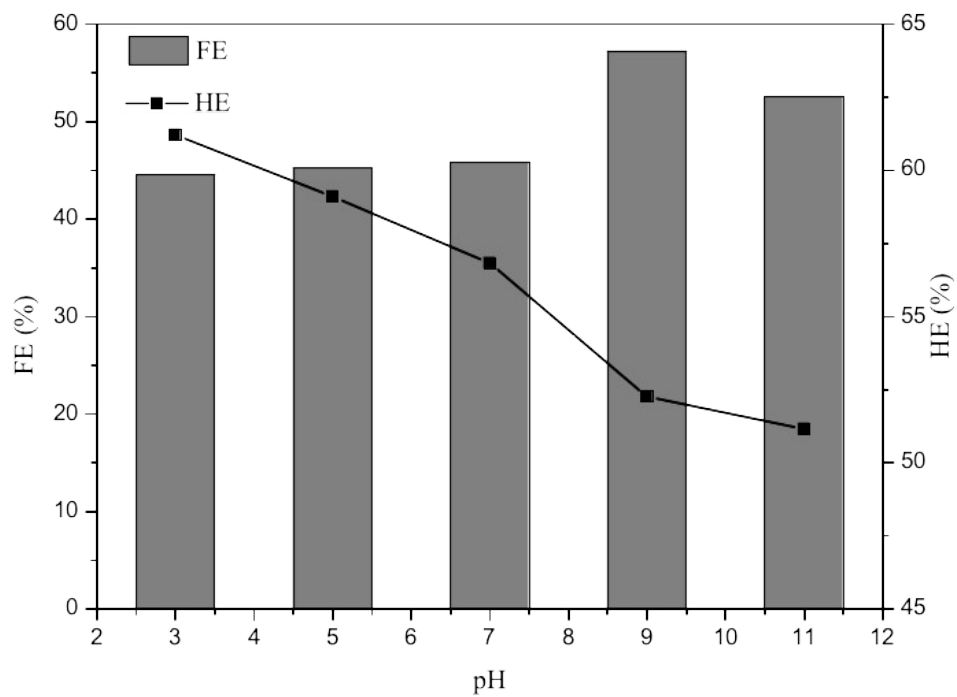
344



345

346 **Fig. 3.** Interaction energies between the flocculants and cells versus the distanced (a:

347 CPAM and *R. glutinis*; b: PAC and *R. glutinis*)



349

350

Fig. 4. pH effect of PAC on *R. glutinis* flocculation

351

352

353

354

355

356

357

358

359

360

361

362

363

364

365

366

367

368

369

370

371

372

373 **List of tables**374 **Table 1** Physico-chemical properties of flocculants and *R. glutinis*

Solid	Dm(μm)	Zeta potential(mV)	Contact angle (°)			
			Water	Ethylene glycol	α-bromonaphthalene	
CPAM	18.6012	Yeast	75.75	118.38	73.33	40.91
PAC	6.773	Yeast	18.20	68.64	70.48	46

375

376 **Table 2** Surface tension energy components of liquid (mJ/m^2) (Good and Van Oss,

377 1992)

Liquid	γ_l	γ_l^{LW}	γ_l^{AB}	γ_l^+	γ_l^-
Water	72.8	21.8	51.0	25.5	25.5
Ethylene glycol	48.0	29.0	19.0	1.92	47.0
α -bromonaphehalene	44.4	44.4	0	0	0

378

379 **Table 3** Surface energy components of flocculants and cells (mJ/m^2)

Solid	γ_s^{LW}	γ_s^+	γ_s^-
CPAM	34.2225(5.85)	0	0
PAC	31.9225(5.65)	0	21.2521(4.61)
<i>R. glutinis</i>	35.6184(5.97)	0.3703(0.61)	0.0198(0.14)

380

381

382 **Table 4**383 **Table 4-1** Influence of CPAM-PAC concentration on FE of *R. glutinis*

PAC CPAM	0.1 g/L	0. 2 g/L	0.25 g/L	0.3 g/L	0.4 g/L
0.4 g/L	50.62	99.84	99.68	99.88	99.57
0.8 g/L	54.68	99.34	99.42	99.89	99.65
1.2 g/L	60.22	99.31	98.28	99.81	99.53
1.6 g/L	63.79	98.58	99.41	99.90	99.81
2.0 g/L	65.76	99.31	99.66	99.93	99.79

384

385 **Table 4-2** Influence of CPAM-PAC concentration on HE of *R. glutinis*

PAC CPAM	0.2 g/L	0. 2 g/L	0.25 g/L	0.3 g/L	0.4 g/L
0.4 g/L	16.43	19.34	18.51	17.97	18.50
0.8 g/L	23.44	25.23	22.63	20.09	21.14
1.2 g/L	37.44	36.11	32.95	22.17	22.69
1.6 g/L	46.95	42.20	38.72	23.77	24.16
2.0 g/L	69.77	50	43.59	28.89	29.73

386